TECHNICAL REPORT ECOM-0339-F

FABRICATION OF ULTRATHIN SOLID ELECTROLYTE BATTERIES

FINAL REPORT
Report No. TO-B 68-31

By
P. Vouros, J. Clune, and J.I. Masters

AUGUST 1968

ECOM
UNITED STATES ARMY ELECTRONICS COMMAND · FORT MONMOUTH, N.J.

CONTRACT DAAB 07-67-C-0339
TECHNICAL OPERATIONS, INCORPORATED
Burlington, Mass.

TECHNICAL REPORT ECOM-0339-F AUGUST 1968

FABRICATION OF ULTRATHIN SOLID ELECTROLYTE BATTERIES

FINAL REPORT

1 APRIL 1967 TO 31 MARCH 1968

Report No. 4

CONTRACT NO. DAAB 07-67-C-0339

Prepared By

P. VOUROS, J. CLUNE, AND J.I. MASTERS

TECHNICAL OPERATIONS, INCORPORATED

BURLINGTON, MASS.

For

U.S. ARMY ELECTRONICS COMMAND, FORT MONMOUTH, N.J.

ACKNOWLEDGMENTS

The authors wish to thank Dr. J.N. Mrgudich for helpful discussions, direct participation in the preparation of this report, and continuing support throughout the program.

ABSTRACT

The objective of this study was to determine the feasibility of preparing solid-electrolyte batteries using only vacuum-deposited thin films. This feasibility has been demonstrated. Batteries were made in two configurations (nonoverlapping and overlapping electrodes). In all cases the anode material was an evaporated Ag film; a variety of electrolytes were studied (evaporated AgI, co-evaporated AgI and KI, evaporated AgBr, a double electrolyte of AgI evaporated onto a film of evaporated $AgC\ell$, a double electrolyte of AgI evaporated onto a film of AgI prepared by iodizing a thin film of Ag previously evaporated onto a film of sputtered Pt); cathode materials were sputtered Pt films (usually) or evaporated Au. Overall cell thicknesses were in the range of 6-12 microns. Preliminary tests indicate that such thin cells are rechargeable and some are apparently of long shelf-life.

PREFACE

The objective of this program was to determine the feasibility of preparing solid-electrolyte batteries using only vacuum-deposited thin films. The approach was to revolve about, but not be limited to, the solid-electrolyte system, Ag/AgI/Pt, proposed by Mrgudich and his colleagues (1) on the basis of work done using thin films of silver and platinum vacuum-deposited on opposite faces of relatively thick (0.25-1.0 cm) pellets of compressed silver iodide powder.

It was realized from the start that the vacuum depositions of silver and platinum films would probably present no serious problems in the fabrication of such all thin-film batteries. The unknown factor was whether techniques could be developed to yield vacuum- deposited films of silver iodide which would be free of pinholes, be adequately good Ag^+ ion conductors and be substantially perfect insulators to electronic flow. Early work clearly indicated that vacuum-deposition of pinhole-free AgI films was, in fact, the major problem and that efforts to improve the ionic conductivity and the electronic resistivity of deposited AgI films would be futile until this pinhole problem was solved.

This report describes three apparently successful approaches to this pinhole problem. Summarized these are:

a. Use of a nonoverlapping electrode configuration whereby a thin film of silver is deposited very close to, but not contacting, a rectangular thin film of platinum; this is followed by evaporation of a film of AgI into the narrow gap separating the two metallic electrodes.

b. An overlapping structure involving evaporation of a thin film of silver bromide (which from past experience we know can be free of pinholes) onto a sputtered film of platinum followed by straightforward evaporation of silver onto the silver bromide. Resultant Ag/AgBr/Pt cells are rechargeable and show open-circuit voltage stability in the charged state.

c. Use of an overlapping configuration in which a sputtered film of platinum is covered with a flash evaporation of silver, followed by conversion through exposure to iodine vapor of this silver film to an apparently adherent pinhole-free film of silver iodide, followed by evaporation of a somewhat thicker film of AgI, followed by evaporation of a film of silver, followed by a dc charging to remove residual un-iodized silver remaining on or in the platinum. Resultant cells are rechargeable and exhibit excellent stability of open-circuit voltage when charged to 0.5 V.

Time has not been available to evaluate long-term shelf-life characteristics of any of these approaches or to optimize design parameters to maximize energy output. Present indications, however, warrant confidence that the overlapping configurations can yield stable and rechargeable cells of about 10 micron (0.0004 in.) thickness.

Mention should be made that the nonoverlapping configuration, adopted originally to sidestep the AgI-pinhole problem, opens the door to thin-film ionic sensors along lines described by Mrgudich (2) who used symmetrical arrays of the type Ag/AgI/Ag to demonstrate that differential deformation or differential heating of the electrodes results in generation of a substantially constant, low-impedance voltage. The nonoverlapping structure permits such differential deformation or heating since the electrodes are physically separated.

TABLE OF CONTENTS

		Page
I.	INTRODUCTION	1
	A. BACKGROUND	1
	B. SOLID-ELECTROLYTE BATTERIES	1
	C. THE Ag/AgI/Pt SOLID-ELECTROLYTE SYSTEM	2
II.	EXPERIMENTAL	4
	A. EVAPORATION PROCEDURES	4
	1. Adoption of Sputtering Techniques for Preparation of Platinum Films	4
	2. Preparation of Evaporated Silver Films	4
	3. Preparation of Evaporated AgI and AgBr Films	4
	4. Protection of Evaporation Equipment Against Corrosion	5
	5. Use of Quartz Substrates	5
	6. Deposition Sequence	5
	B. ELECTRICAL CIRCUITS	5
	1. Battery Charge-Discharge Circuit	5
	2. Resistance Measurements	6
	C. CELL CONFIGURATIONS	6
	1. The Overlapping Configuration	6
	2. The "Nonoverlapping" Configuration	8
	D. RESULTS OBTAINED WITH NONOVERLAPPING Ag/AgI/Pt CELLS	8
	1. Behavior of Open-Circuit Voltage During Evaporation	8
	2. Discharge Behavior of the Nonoverlapping Ag/AgI/Pt Cell	9

TABLE OF CONTENTS (Cont'd.)

Page

3. Improvement of Nonoverlapping Behavior Using More Conductive Solid-Electrolyte Materials 10

4 An Interesting By-Product of the Nonoverlapping Configuration (Thin Film Sensors) 12

E. OVERLAPPING Ag/AgBr/Pt CELLS 12

F. OVERLAPPING Ag/AgBr/Au CELLS 13

G. OVERLAPPING Ag/AgI, AgCℓ or AgBr/Pt CELLS 13

H. ELIMINATION OF PINHOLES IN EVAPORATED AgI FILMS 15

1. Introduction 15

2. Effect of Substrate Temperature on the Continuity of Evaporated AgI Films 15

3. A Stable Overlapping Ag/Evap. AgI, Iodized Ag/Pt Cell . . . 17

III. DISCUSSION 22

A. FUNDAMENTAL NATURE OF THE Ag/AgI/Pt SYSTEM 22

B. SIGNIFICANCE OF AN EXPONENTIALLY-DROPPING CLOSED-CIRCUIT VOLTAGE 23

C. MINIMIZING THE DROPPING CLOSED-CIRCUIT VOLTAGE . . 23

D. DEVELOPMENT OF THIN-FILM, ALL-SOLID OXIDATION-REDUCTION SYSTEMS 23

IV. CONCLUSIONS 24

A. THIN-FILM BATTERIES 24

B. THIN-FILM SENSORS 24

V. RECOMMENDATIONS 25

APPENDIX A. ELECTRICAL MEASUREMENTS 26

INTRODUCTION 26

AC AND DC CHARACTERISTICS OF THIN-FILM CELLS 29

CONCLUDING REMARKS 33

REFERENCES 35

LIST OF ILLUSTRATIONS

Figure		Page
1	Basic Circuit Diagram	6
2	Schematic of Overlapping Configuration	7
3	Schematic of Nonoverlapping Cell Configuration	8
4	Nonoverlapping Pt/AgI/Ag Cell OCV as a Function of AgI Evaporation	8
5	Discharge Curves of Nonoverlapping Pt/AgI/Ag Cell	10
6	Discharge Curves for Nonoverlapping $Pt/KAg_4I_5/Ag$ Cell	11
7	Electron Micrograph of Evaporated AgBr Film (Magnification 12,000X)	12
8	Overlapping Ag/AgBr/Pt Cell OCV as a Function of Evaporated Ag Deposition	13
9	Discharge Curves for Overlapping Ag/AgBr/Pt Cells Using Various Loads	14
10	Discharge Curves for Overlapping Ag/AgBr/Au Cells Using Various Loads	15
11	Discharge Curves for Overlapping Ag/AgI, AgCℓ/Pt Cell at Various Temperature (R_L = 1 MΩ)	16
12	Electron Micrographs of AgI Films Deposited at Different Substrate Temperatures	18
13	Typical Charging Curve for Overlapping Ag/Evap. AgI, Iodized Ag/Pt Cell	20
14	Discharge Curves for Overlapping Ag Evap. AgI, Iodized Ag/Pt Cell	21
15	Sample Circuit Analogue of Cell	26
16	AC Bridge for Conductivity Measurements	30
17	Transient Response of an Ag/AgBr/Ag Thin-Film System to a 10 mV Step Using Various Loads Large Compared with Electrolyte Resistance	31

I. INTRODUCTION

A. BACKGROUND

Rapid progress is being made by the electronics industry to miniaturize electronic components, circuits and systems. In many instances such miniaturization has resulted in sharp reductions in power requirements. Indeed, a recent RCA announcement (3) describes metal oxide semi-conductors operating on nanowatts in the quiescent state, using greater power only during the instant of information switching. It seems inevitable that these emerging smaller and more sensitive electronic circuits will call for equivalent miniaturization of the batteries required to power them.

The primary battery industry, which conventionally uses aqueous solutions as the ionically-conductive, electronically insulative interface separating the battery anodic and cathodic electrodes, has been responsive to this miniaturization trend. The smallest conventional battery as of today (the Ruben-Mallory 212 cell) has a volume of only 0.085 cm^3. Further miniaturization of conventional, liquid-electrolyte primary batteries is probably possible, but problems of manufacturing control and long-term containment of liquid electrolytes become more and more formidable as cell size decreases and will eventually impose a lower limit (probably at about 0.05 cm^3 per cell) below which the liquid-electrolyte approach to battery miniaturization will become impractical.

It was in anticipation of a future need for cell volumes in the range of 0.001-0.05 cm^3 per cell that this study of ultra-thin cells was instituted under the sponsorship of the Institute for Exploratory Research, U.S. Army Electronics Command, Fort Monmouth, N.J.

B. SOLID-ELECTROLYTE BATTERIES

Many solids are known which, like aqueous solutions, are ionic conductors and electronic insulators. For example, under an applied field and between silver electrodes, a current will flow through a compressed pellet of silver iodide powder and all of the current is due to transport of silver ions. Many other solids exhibit such ionic flow and electronic insulation. In addition it has been well established that the electrochemistry of such solid "electrolytes" is quite analogous to the electrochemistry of aqueous electrolytes (4). This analogous behavior leads directly to the concept of solid-electrolyte batteries. The concept is intriguing from the standpoint of battery miniaturization since such solid electrolytes, unlike liquid electrolytes, should be amenable to easy, precise and permanent positioning within the tiny cell structure, thus neatly avoiding the electrolyte control and containment problems associated with miniature batteries using liquid electrolytes. In addition such all-solid batteries could be made very resistant to shock, vibration or spin and should be operable over a wider temperature range since they contain no aqueous electrolytes which can freeze or boil away.

Several serious efforts were made in the late 1950's to develop such miniature solid-electrolyte batteries. These are summarized in Reference (5). Although these efforts confirmed predictions concerning small size, ease of manufacture, good shelf-life, rugged structures and wider operational temperature range, high internal resistance and high polarization losses entered to limit useful output even at fractional microampere drains.

These high internal losses on discharge were generally attributed to the well-known fact that the room-temperature ionic conductivities of even the most conductive solid electrolyte known at that time (e.g., solid silver iodide) were several orders of magnitude less than those of most aqueous liquid electrolytes. Although this argument is valid, it represents only a part of the story. One can easily envision a situation where even if the solid electrolyte had a much higher ionic conductivity, the overall battery system would still exhibit low useful output. For example, consider the National Carbon Ag/AgI/V_2O_3 system (6). On discharge, silver ions should be free to enter and diffuse through the AgI electrolyte and be free to enter and permeate through the V_2O_3 cathodic mass. Thus, the cathodic mass should also be a good conductor for silver ions. The Union Carbide design incorporated AgI powder into the cathodic mass to help this entry of silver ions. But this at best just brings the Ag^+ ion to the surface of the V_2O_3 grain. Furthermore, the cathodic mass should also be an electronic conductor to permit easy acceptance of charge-compensating electrons entering from the external circuit during discharge. The Union Carbide design incorporated electronically conductive acetylene black into the cathodic V_2O_3 — AgI mass, but again this merely brings the electron to the surface of the V_2O_3 grain and does not insure electronic assimilation into the grain.

Such deterrents to free Ag^+ ion entry into the AgI electrolyte, easy movement through the AgI and easy entry and permeation of Ag^+ ions and electrons into the cathodic mass detract from useful battery output.

C. THE Ag/AgI/Pt SOLID-ELECTROLYTE SYSTEM

As pointed out in Reference (1), the initial impetus to study of the battery behavior of a thin Ag film/0.1 cm thick AgI pellet/thin Pt film 1.27 cm diameter system was the observation that the "flash" current (i.e., the maximum momentary current on substantially dead short) was about 100 microamperes per cm^2 of cross-sectional electrode area. This qualitative reciprocal measure of battery internal resistance was at least three times better than that of the best of previously described major solid-electrolyte systems. Use of thinner pellets (0.025 cm) and system charging to 0.6 V resulted in flash currents (through a 150 ohm passive Gierback microammeter) of 600-700 microamperes/cm^2. These high flash currents were encouraging evidence of possible sharp improvement in the useful output of all-solid batteries. Even further impetus is derived from the fact that the Ag/AgI/Pt system is capable of repeated recharge.

An intriguing feature of the Ag/AgI/Pt system is that, in principle at least, all of the components may be amenable to thin-film vacuum-deposition techniques, with sharply increased design flexibility. Such deposition of the Ag and Pt metallic

components should present no really serious problems. The big unknown factor is vacuum deposition of the AgI film. Such films should be free of pinholes, permit Ag^+ ion flow and block electronic flow. A vast amount of previous Technical Operations experience with vacuum-deposition of AgCℓ and AgBr films indicated pinhole-free characteristics with these compounds, but it was not certain that this necessary condition could be achieved with AgI.

The primary objective of this contract was to determine the feasibility of preparing Ag/AgI/Pt batteries using only vacuum-deposited thin films. The following sections describe our work.

II. EXPERIMENTAL

A. EVAPORATION PROCEDURES

1. Adoption of Sputtering Techniques for Preparation of Platinum Films

Since preparation of platinum films by evaporation, although fast, requires very high temperatures (usually involving electron-beam heating) and since radiation-heating of AgI could be harmful, it was decided to adopt the slower but lower temperature, sputtering technique for all Pt deposition. A consolidated Vacuum Corporation AST-100 low energy sputtering unit was purchased and installed. Normally, sputtering was done at a pressure of 2×10^{-3} mm Hg, a filament current of 48 A, an anode current of 3.5 A and an anode voltage of 40 V. The target voltage was set at 600 V and the target to substrate distance was approximately 15 cm. Under these conditions platinum films of a thickness of 500-700 Å were deposited in approximately 1/2 hour of sputtering time. Platinum films measuring 2.5 cm long and 0.63 cm wide (usual size) had ohmic resistances in the 50-60 ohm range.

It might be added here that another reason for the purchase of the sputtering unit involved the possibility that techniques for deposition of sputtered AgI films might be developed. Time was not available to us to try this approach.

2. Preparation of Evaporated Silver Films

Silver films were deposited by evaporation of silver at a bell-jar pressure of approximately 5×10^{-5} mm Hg. A heated, coiled tantalum filament was used to hold the silver sample and the deposited silver films were 2.5 cm long and 0.63 cm wide and had ohmic resistances in the 20-30 ohm range.

3. Preparation of Evaporated AgI and AgBr Films

Films of AgBr and AgI varying in thickness from 5-12 microns were deposited by heating the material in tungsten boats at a pressure of 5×10^{-5} mm Hg. Boat temperatures were kept constant during the deposition at 632°C for AgBr and 560°C for AgI. Evaporation rates for the AgBr and AgI were approximately 0.75 μ/min and 0.3 μ/min respectively.

An interference measurement technique was used to determine the thickness of the AgBr film by placing a flat triacetate film next to the substrate as a reference during the evaporation (7). A gravimetric method based on the bulk density of AgI was used to estimate the thickness of the deposited AgI film. (Note: the values for the thickness of the AgI films may be subject to a 30% error since our work on evaporated AgBr films, whose measured density 4.55 g/cm^3 is much less than the true density of 6.5 g/cm^3, indicates that the density of evaporated silver halide films is appreciably lower than the bulk density.)

4. Protection of Evaporation Equipment Against Corrosion

Because of the corrosive effects of iodine vapors produced during the AgI evaporations and of possible reaction of AgI with more active metals (e.g., $A\ell + 3AgI = 3Ag + A\ell I_3$), all copper-coated sections of the evaporator were nickel-plated or replaced with stainless steel. The vapors were further contained by conducting the evaporations within a small bell jar housed inside the main bell jar of the unit. These precautions also tended to minimize corrosion of the sputtering equipment.

5. Use of Quartz Substrates

Initial work used glass substrates, but this was quickly changed to universal use of quartz substrates when evidence was obtained of erratic cell voltages when using glass (due presumably to some conductivity of glass).

6. Deposition Sequence

The previous section mentioned the presence of free iodine vapor during the AgI evaporations. These vapors are noticeably more pronounced during the early stages of the evaporation. Attempts to evaporate AgI onto a previously evaporated Ag film resulted in an increase of the resistance of the Ag film (unless it was quite thick) because of its reaction with the iodine vapors. Although this attack of iodine on this silver film is probably inhibited by the protective action of an initially formed AgI film, the observation that the resistance of a sputtered Pt film was unaffected by the action of iodine vapors led to adoption of a Pt-AgI-Ag deposition sequence.

B. ELECTRICAL CIRCUITS

1. Battery Charge-Discharge Circuit

The circuit shown in Figure 1 was used to study the charge and discharge characteristics of fabricated experimental cells. Excluding the cell itself, the power supply for charging and the recorder, all switches, plug-in jacks and resistors were assembled on a 1/4 inch thick teflon board to keep spurious leakage currents at a minimum. The power supply was voltage-regulated to provide a constant charging voltage of 0.5 V and this value was used in all charging experiments unless otherwise specified. A Keithley 610B electrometer with 10^{14} ohms input impedance was used to monitor charging currents by measuring the IR drop across a 1000-ohm resistor and for monitoring cell discharge voltages at different discharge loads (usually 0.1, 0.5, 1.0, and 10 megohms). The Keithley electrometer output was recorded with a Bausch and Lomb VOM-5 recorder.

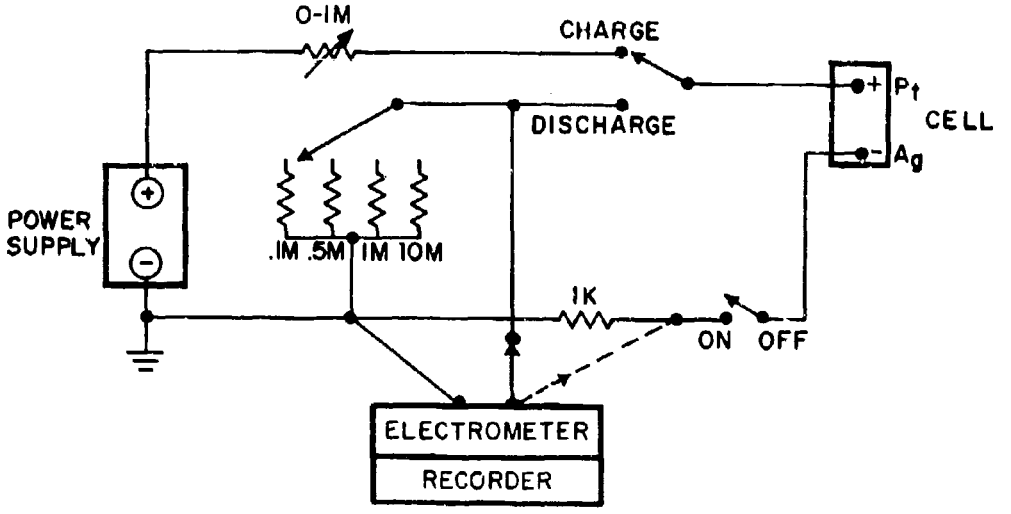

Figure 1. Basic Circuit Diagram

2. Resistance Measurements

Attempts to measure electrolyte and/or cell resistances were made to develop clearer insight concerning the major factor entering to impede ionic transport through the cell system. Resistance data were obtained by the three methods (ac bridge, determination of matching load resistor required to drop starting open-circuit voltage to one-half, and "initial voltage drop" estimation. In order to avoid the possibility that such analysis might becloud our primary objective -- to evaluate the feasibility of fabrication of stable and rechargeable thin-film batteries — the discussion of electrical measurements is presented in detail in Appendix A.

CELL CONFIGURATIONS

1. The "Overlapping" Configuration

This structure, illustrated in Figure 2, sandwiches the evaporated AgI between crossed films of sputtered Pt and evaporated Ag. Initial work with this configuration, using auxiliary leads to monitor cell voltage during deposition of the final silver film, showed quite conclusively that only a very small amount of silver could be deposited before a slowly rising cell voltage (usually not in excess of 0.3 V) suddenly dropped and stayed at zero. This was interpreted as indicative of pinholes in the AgI film through which evaporated Ag threads could reach the Pt film with resultant internal electronic short circuit. We were unsuccessful in our initial efforts to eliminate this pinhole shorting and turned to a "nonoverlapping" configuration whose design could tolerate electrolyte pinholes.

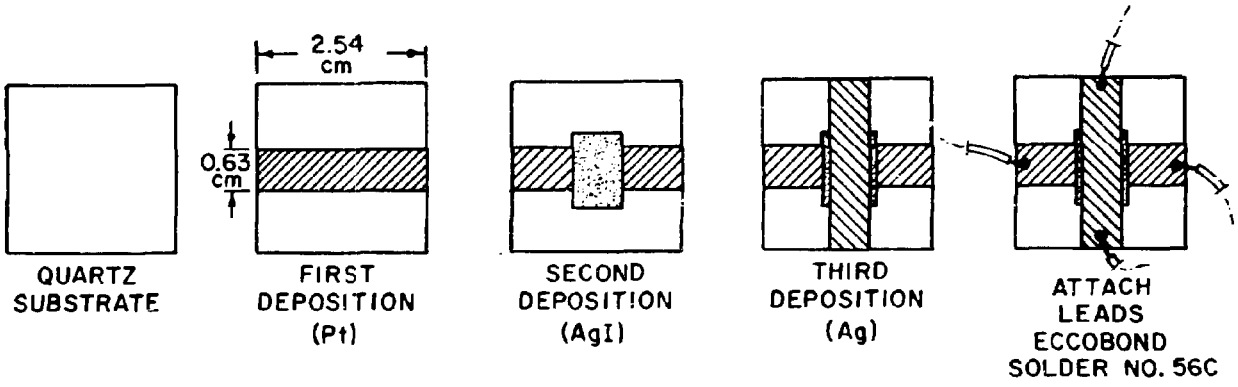

Figure 2. Schematic of Overlapping Configuration

2. The "Nonoverlapping" Configuration

This structure, whose initial deposition sequence is illustrated in Figure 3, deposits a sputtered Pt film using an appropriate mask to yield a sharp, straight edge. This Pt film is then mashed and a thin silver film with a corresponding sharp, straight edge is deposited very close to, but not touching, the straight edge of the Pt film. The resulting narrow gap between the Pt and Ag films is then filled by an AgI evaporation. Subsequent work changed the deposition sequence to Pt-AgI-Ag to avoid the attack of initially evolved iodine vapor during the AgI evaporation upon a previously deposited Ag film as discussed in Section II-A-6 above. This change to a Pt-AgI-Ag deposition sequence did not change the overall initial behavior of the cell but did improve its OCV stability. Even in this sequence, however, several months storage did show some tendency for a slow disappearance of the Ag film which could be due to the presence of excess contrapped iodine in the AgI or possibly oxidation by air to Ag_2O, or possibly to diffusion of free metallic silver atoms along and into the voids known to exist in the evaporated AgI films prepared in this manner.

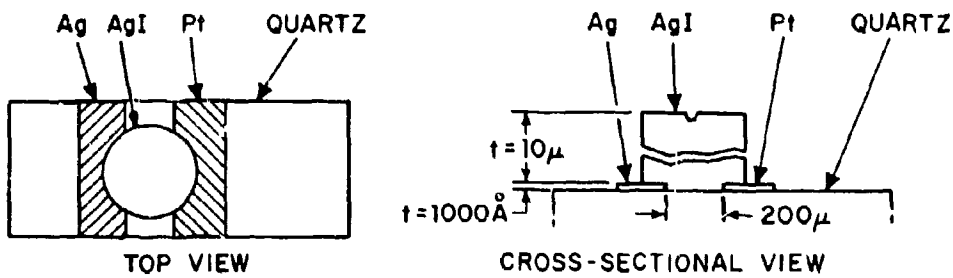

Figure 3. Schematic of Nonoverlapping Cell Configuration

D. RESULTS OBTAINED WITH NONOVERLAPPING Ag/AgI/Pt CELLS

1. Behavior of Open-Circuit Voltage During Evaporation

The rate of increase of monitored cell voltage as a function of AgI evaporation using the initial Pt-Ag-AgI deposition sequence is shown in Figure 4. There was no

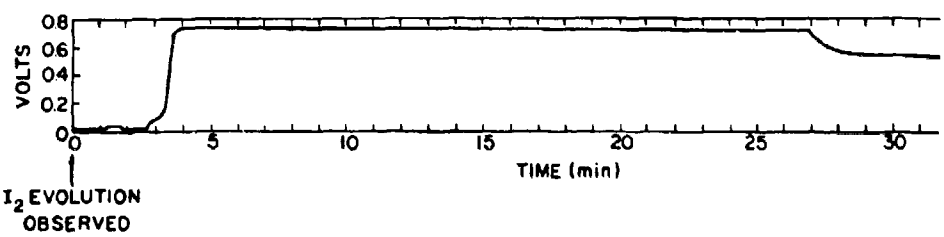

Figure 4. Nonoverlapping Pt/AgI/Ag Cell OCV as a Function of AgI Evaporation

significant voltage increase for more than 2.5 minutes after iodine evolution was first observed during heating of the AgI boat. This was followed by a gradual increase in cell voltage presumably due to a gradual buildup of the silver iodide within the gap between the Pt and Ag electrodes. Another possible reason for this slow increase in cell voltage is that the initial impedance of the first very thin bridging film of AgI probably exceeds that of the electrometer itself. The cell voltage finally reached a value of 0.725 V, where it remained constant for the duration of the 27-minute evaporation of AgI. The evaporation heater was then turned off and the cell voltage slowly dropped to 0.550 V where it remained constant even after the system had been vented to the atmosphere.

Although we are tempted to explain the 0.725 open-circuit voltage during evaporation as being due to the presence of free iodine at the Pt electrode which could result in an $Ag/AgI/I_2$, Pt oxidation-reduction system (known to have an OCV of about 0.69 V at room temperature and, possibly, 0.725 at the higher substrate temperature during evaporation), such an explanation ignores the fact that the iodine evolved during evaporation is also available at the Ag electrode. We can, however, postulate that the iodine at the silver electrode (which in this early case was deposited before the AgI evaporation reacts with the silver to form AgI in which case the $Ag/AgI/I_2$, Pt explanation is more tenable.

The drop to 0.55 V after the evaporation was stopped is understandable on the basis that continued pumping sucked off the excess iodine, causing the cell to assume the lower concentration cell voltage of the Ag/AgI/Pt system.

2. Discharge Behavior of the Nonoverlapping Ag/AgI/Pt Cell

It is obvious that the nonoverlapping configuration is bound to yield cells of very high resistance. One reason is that the open gap between Pt and Ag must, because of mechanical difficulties of marking, be relatively large at about 200 microns. A second reason is that "facing" electrode areas must be small (1000 AU x length of evaporated AgI). The "effective" electrode area, which is greater because some Ag^+ ion transport can be through upper portions of the AgI films, is probably not too beneficial since such circuitous Ag^+ ion transport is along longer paths.

Nevertheless, the nonoverlapping cell should be stable, exhibit battery output and in addition, should be rechargeable. Battery discharge characteristics under different loads are shown in Figure 5. In all cases, after the discharge run, the cell was recharged under 0.5 V for one hour. (Note: output performance could be significantly improved if, as Reference (1) points out, we charged under 0.6 V for three days, but our contract time was limited and our objective was to demonstrate feasibility of design, cell stability, battery behavior and rechargeability. Time was not available for us to study optimization of output, even though there are several rather obvious ways in which this can be accomplished.)

Referring to Figure 5, one conventional way to make a rough estimation of battery internal resistance, r, is by means of the easily derived expression that $r = (E-V)R/V$, where E is the open-circuit voltage and V is the "instantaneous" closed-circuit voltage when the cell is placed across an external resistance, R_L.

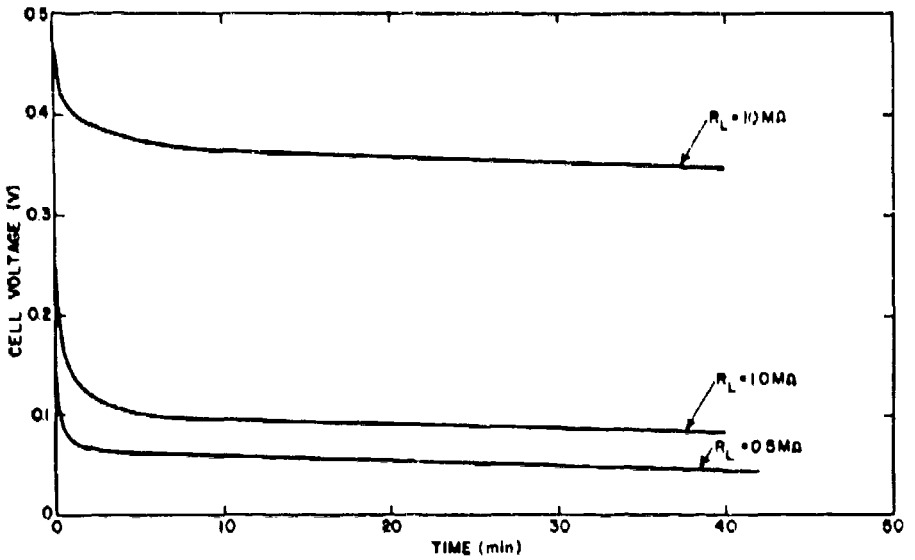

Figure 5. Discharge Curves of Nonoverlapping Pt/AgI/Ag Cell

The "instantaneous" condition (never realized in practice) is involved to avoid polarization losses which enter to further depress the closed-circuit voltage. In Figure 5, the quantity V is 0.46 at $R_L = 10^7$, 0.24 when $R_L = 10^6$ and 0.14 when $R_L = 5 \times 10^5$. These values, when substituted in the above expression using E = 0.5 V, yield "r" values of 0.9×10^6, 1.1×10^6 and 1.3×10^6. This represents adequate, but probably fortuitous, reproducibility.

3. Improvement of Nonoverlapping Behavior Using More Conductive Solid-Electrolyte Materials

Very recent work by Bradley and Greene in England (8), and Owens, Argue, Geller and Grace of Atomics International (9-11), has indicated that certain double salts of AgI of the general form MAg_4I_5 (where M is an alkali such as K, Rb, NH_4 or, to a limited extent, Cs) exhibit Ag^+ ion conductives several order of magnitude higher than AgI. We made a very preliminary and qualitative attempt to take advantage of these higher conductivities using the nonoverlapping configuration.

The starting material was a 1:4 molecular ratio of KI and AgI corresponding to the compound KAg_4I_5. This mechanical mixture was pretreated as described in Reference (9) i.e., mixed, melted, quenched, ground, and annealed at 165°C for 16 hours. It was then evaporated from a tungsten boat at 480°-490°C at 5×10^{-5} mm Hg into the Pt-Ag gap of the nonoverlapping configuration. The monitored voltage-time curve was identical with that of Figure 4, including the iodine evolution effect.

The cell, which we shall here designate as $Ag/KAg_4I_5/Pt$ (even though we undoubtedly did not have stoichiometric KAg_4I_5), was then charged and discharged as in the case of the Ag/AgI/Pt nonoverlapping cell of Section II-D-2 above. The discharge curves obtained are illustrated in Figure 6. Applying the $r = (E-V) \times R/V$ expression to these curves we find that V was 0.48 at $R = 10^6$, 0.45 at $R = 5 \times 10^5$ and 0.36 at $R = 1 \times 10^5$. Calculated values for r, the internal resistance, were 4.2×10^4 ohms at $R = 10^6$, 11×10^4 at $R = 5 \times 10^5$ and 40×10^4 at $R = 1 \times 10^5$. Although more erratic (probably due to entry of increased polarization effects at higher drains), these resistances are lower by more than two orders of magnitude than with the Ag/AgI/Pt system.

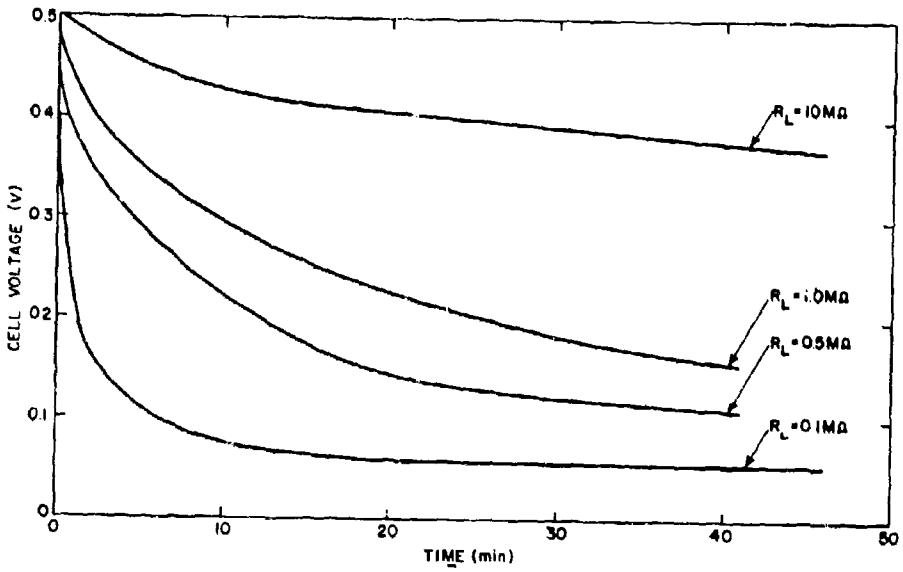

Figure 6. Discharge Curves for Nonoverlapping $Pt/KAg_4I_5/Ag$ Cell

Open circuit voltage stability of these KAg_4I_5 cells, however, was unsatisfactory, beginning to deteriorate after but a few days storage. This is probably due to some electronic conductivity associated with non-perfect stoichiometry of the electrolyte. For example, assume that the KAg_4I_5 lattice was deficient in I^- ions, yielding a compound of the type KAg_4I_{5-x}. Charge compensation requires that electron be present to compensate for the lost I^- ions. The presence of such electrons, depending on their mobility, may impart deteriorating internal electronic conductivity to the cell system.

Recognizing the importance of electrolyte stoichiometry, it is likely that non-electronically conductive but better ionically conductive, thin film cells can be fabricated in the nonoverlapping electrode format. Time, however, was not available to pursue this important avenue.

4. An Interesting By-Product of the Nonoverlapping Configuration (Thin-Film Sensors)

Mrgudich, at the 1967 Power Sources Conference Atlantic City, reported on ionic sensors, one example of which was a symmetrical Ag/AgI pellet/Ag array. If such an array is bent, one Ag electrode is stretched and the other compressed. These different strains apparently change the originally equal silver electrode potentials by different amounts so that bending spontaneously generates a fairly stable output voltage, representing the difference in such deformation-induced electrode potentials. Furthermore, heating one silver electrode and not the other also generates a voltage. Such sensing capabilities depend upon a significant separation of the electrodes. A symmetrical nonoverlapping Ag-AgI-Ag thin-film array would permit us to do substantially equivalent sensing by stress or temperature disturbance of one electrode and not the other. In a personal communication Mrgudich reported a differential deformation sensing voltage output of one of our thin-film nonoverlapping Ag/AgI/Ag arrays.

E. OVERLAPPING Ag/AgBr/Pt CELLS

Previous experience at Technical Operations had shown that AgBr could be evaporated onto unheated substrates to yield pinhole-free thin films with thicknesses even as low as about 0.2 microns (see Figure 7). Although the Ag^+ ion conductivity of AgBr is some two or so orders of magnitude less than that of AgI and although the literature reports some trace of electronic conductivity in AgBr (especially in the presence of free bromine), the pinhole-free advantage was considered sufficiently important to warrant some exploration of the Ag/AgBr/Pt thin-film system.

Figure 7. Electron Micrograph of Evaporated AgBr Film (Magnification 12,000X)

A thin-film overlapping Ag/AgBr/Pt cell was prepared in the configuration of Figure 2, i.e. sputtered Pt on quartz, followed by a 5-10 micron layer of evaporated AgBr, followed by an evaporation of silver. The silver evaporation was monitored as described above; the monitoring open circuit voltage results are illustrated in Figure 8.

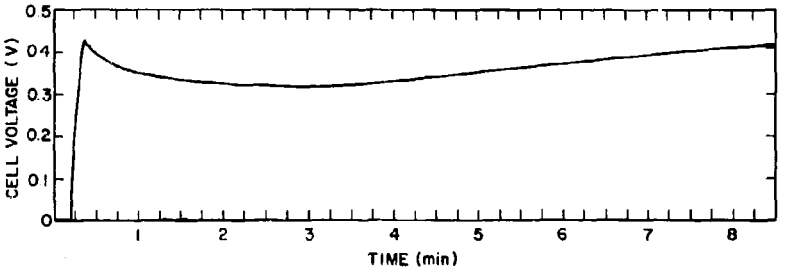

Figure 8. Overlapping Ag/AgBr/Pt Cell OCV as a Function of Evaporated Ag Deposition

The overlapping Ag/AgBr/Pt cell was then charged under 0.5 V and subjected to a series of discharge-charge cycles whose results are illustrated in Figure 9. Applying, as before, the expression that the nearly polarization-free internal resistance, r, of the cell is given by (E-V) x R/V, we have that V = 0.45 when R was 10^7 ohms, 0.41 at R = 10^6, 0.29 at R = 5 x 10^5 and 0.18 at R = 1 x 10^5. Corresponding values of r are: 1.1 x 10^4 ohms at R = 10^7, 2.2 x 10^3 at R = 10^6, 3.6 x 10^5 at R = 5 x 10^5 and 1.6 x 10^5 at R = 10^5. We have no immediately plausible explanation for the erraticism (most pronounced in the 2.2 x 10^3 ohm value at R = 10^6 ohms), although it is possible that the silver film was not thick enough to remain continuous during the discharge cycles.

F. OVERLAPPING Ag/AgBr/Au CELLS

We also prepared Ag/AgBr/Au cells in the overlapping configuration. The discharge-charge curves are shown in Figure 10. Output characteristics are relatively lower than for the Ag/AgBr/Pt cell of Figure 9.

G. OVERLAPPING Ag/AgI, AgCℓ or AgBr/Pt CELLS

In an attempt to overcome the problem of pinholes observed with evaporated AgI films we decided to deposit a thin layer (approximately 0.625 micron) of AgCℓ or AgBr over the sputtered Pt film, followed by evaporation of a thicker (approximately 5 micron) film of AgI, followed by deposition of the anodic Ag film. Such double-electrolyte cells exhibit a high internal resistance (about 4 x 10^7 ohms when measured by estimation of the external resistance required to give a closed-circuit voltage equal to one-half the original 0.5 V charged open-circuit voltage). These cells exhibited excellent open-circuit voltage retentions on the 0.5 V charged condition.

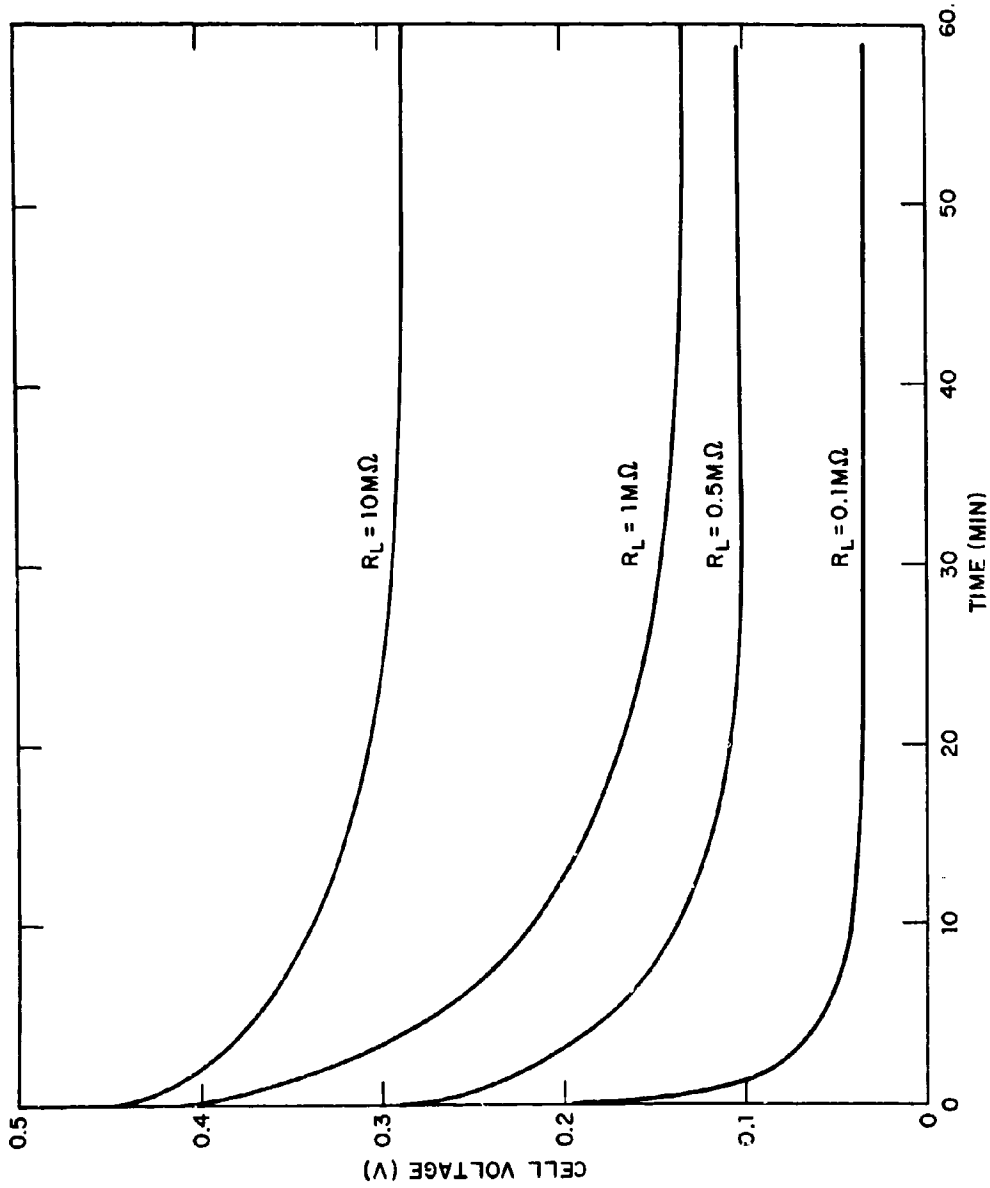

Figure 9. Discharge Curves for Overlapping Ag/AgBr/Pt Cells Using Various Loads

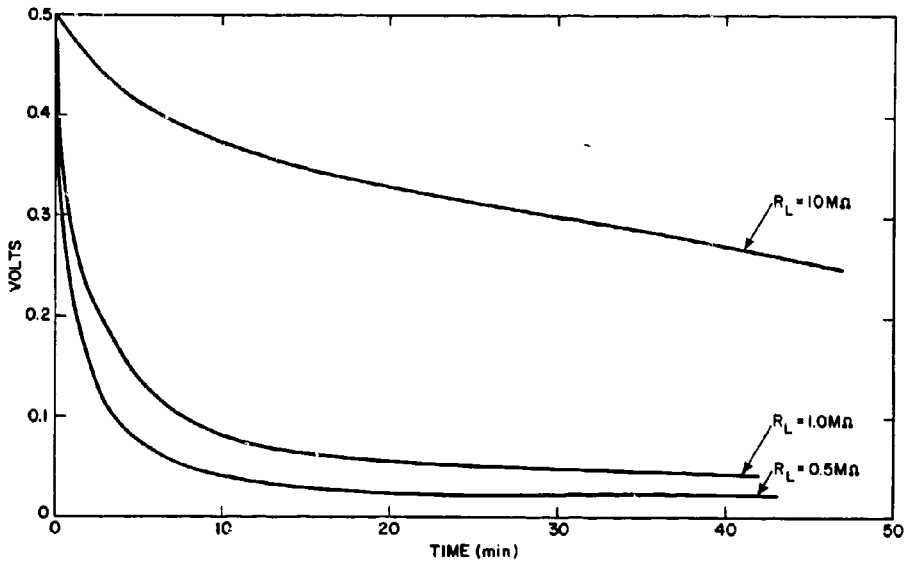

Figure 10. Discharge Curves for Overlapping Ag/AgBr/Au Cells Using Various Loads

A typical Ag/AgI, AgCℓ/Pt cell was discharged at various temperatures, always across a 1 megohm load. The rather interesting discharge curves of Figure 11 were obtained. These demonstrate discharge-charge capability at elevated temperatures, and this capability is increased with temperature presumably due to an increase in the larger number of active sites available for adsorption and/or absorption of silver atoms at the platinum electrode. However, the increased ionic conductivity of the electrolyte, and the increased rate constant of the electrode reactions at higher temperatures, may also have contributed to the improved energy capacity of the cell.

H. ELIMINATION OF PINHOLES IN EVAPORATED AgI FILMS

1. Introduction

In a fundamental sense, all of the above efforts represent attempts to dodge the troublesome pinholing effect observed whenever we tried to evaporate a film of AgI. It was only during the latter stages of this contract that we were able to develop a direct and apparently successful approach to this basic problem.

2. Effect of Substrate Temperature on the Continuity of Evaporated AgI Films

Anticipating that higher substrate temperatures might increase the physical mobility of evaporated AgI film, we set up procedures whereby we could use electron microscope techniques to follow the physical structure of films of AgI deposited

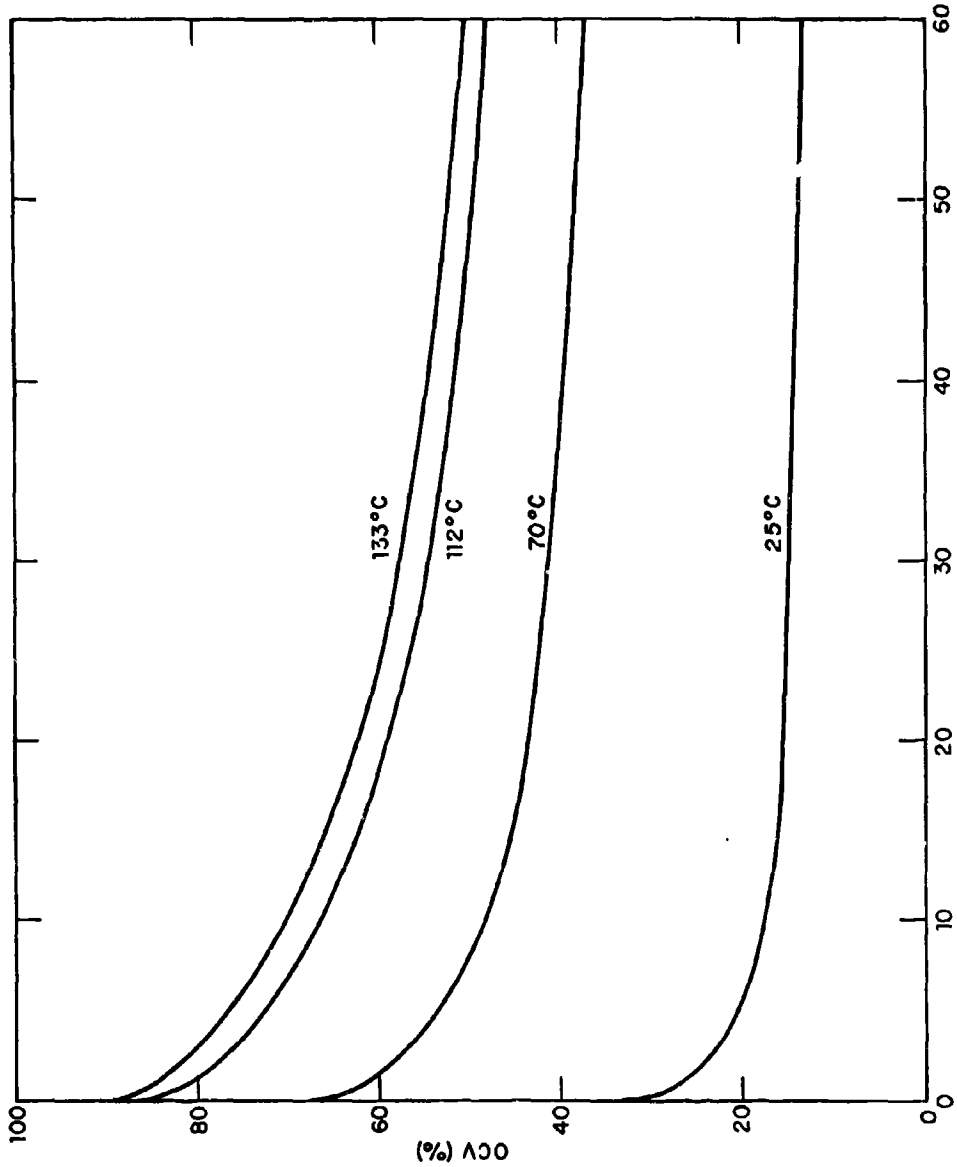

Figure 11. Discharge Curves for Overlapping Ag/AgI, AgCℓ/Pt Cell at Various Temperatures (R_L = 1 MΩ)

at different substrate temperatures. This technique involved evaporation of AgI onto thin (electron-transparent) carbon films supported on conventional nickel grids used in electron microscopy. The AgI evaporation procedure was identical to that used for AgI film evaporation directly onto quartz substrates except that the temperature of the carbon-coated nickel grids was varied. After evaporation of the AgI, the film was shadowed at a 3:1 angle using a platinum-imbedded carbon pellet technique. The film was then coated at normal incidence with carbon and the AgI film (opaque to an electron beam) removed by dissolving it in a methanolic KCN solution (0.5 gm KCN/50 mℓ CH_3OH). The resultant replica of the original AgI film was then gently washed for 5 minutes in three changes of distilled water.

Figure 12a illustrates voids in an AgI film deposition at a substrate temperature of 41°C. Figure 12b is an unreplicated, straight transmission of the unremoved AgI film. This shows that these voids extend all the way through the AgI film. Although there is a pronounced change in structure at 100°C (Figure 12c), voids are still present, at higher substrate temperatures (Figure 12d at 150°C, Figure 12e at 175°C, and Figure 12d at 200°C) these voids disappear and stay disappeared, even when the sample is subsequently cooled to room temperature for electron microscope examination.

A possible explanation for this encouraging tendency to eliminate voids with substrate temperatures above 150°C could be related to the fact that AgI above 145°C exists as an alpha-phase (12). When the temperature drops below 145°C this alpha-phase transforms, with a 5.4% expansion (13), into a beta-phase, stable between 138°-145°C, but metastable at room temperature. Such expansion would of course contribute to closing of voids (if indeed they exist at 200°C) as the substrate is cooled to room temperature.

3. A Stable Overlapping Ag/Evap AgI, Iodized Ag/Pt Cell

In view of these encouraging results concerning elimination of voids in AgI films we reinstituted efforts to develop a stable, overlapping Ag/AgI/Pt cell.

A strip of Pt film 2.5 cm long x 0.63 cm wide with a resistance of 40 ohms was sputtered onto the quartz substrate. This was followed by deposition of a film of silver approximately 1000 Å thick over the central portion of the Pt. The sample was then placed in an iodine chamber for about 24 hours to convert most of the silver to AgI. Such iodizing, similar to that used in the National Carbon $Ag/AgI/V_2O_5$ system (6), should result in an adherent, continuous, protective AgI film. A layer of evaporated AgI was then deposited over the iodized AgI film and this, in turn, was followed by deposition of a 2.54 cm x 0.63 cm Ag film in the "cross" configuration (Figure 2) of the overlapping geometry. Cell voltage was monitored in vacuum during the Ag deposition; it never rose above 0.05-0.06 V, presumbably due to the presence of some silver at the Pt electrode surface.

(a). 41°C

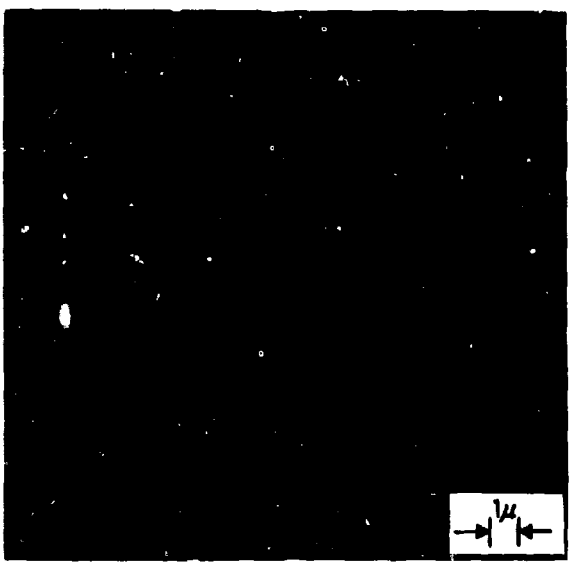

(b). 41°C (Shadowgraph)

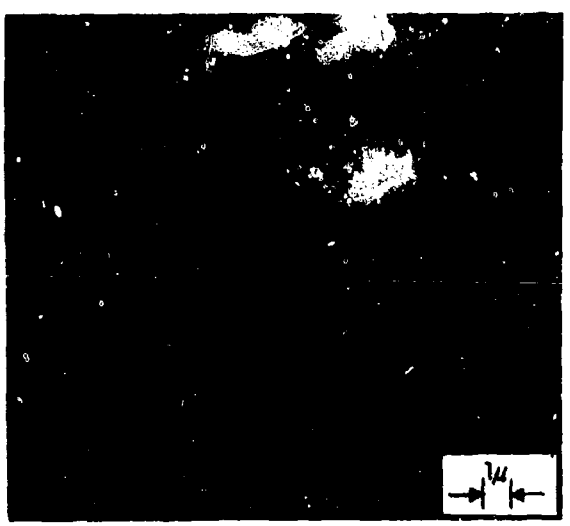

(c). 100°C

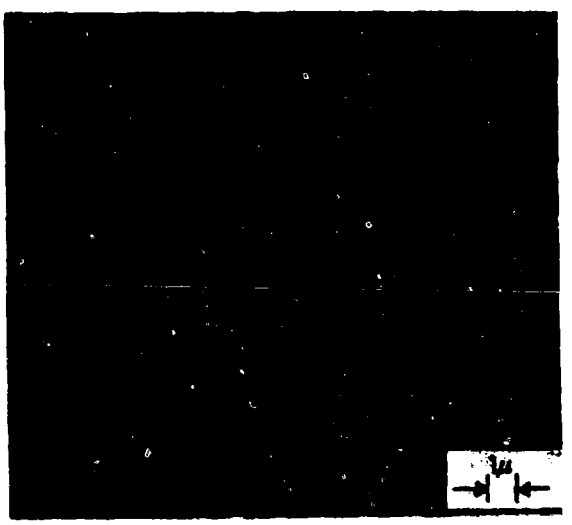

(d). 150°C

Figure 12. Electron Micrographs of AgI Films Deposited at Different Substrate Temperatures

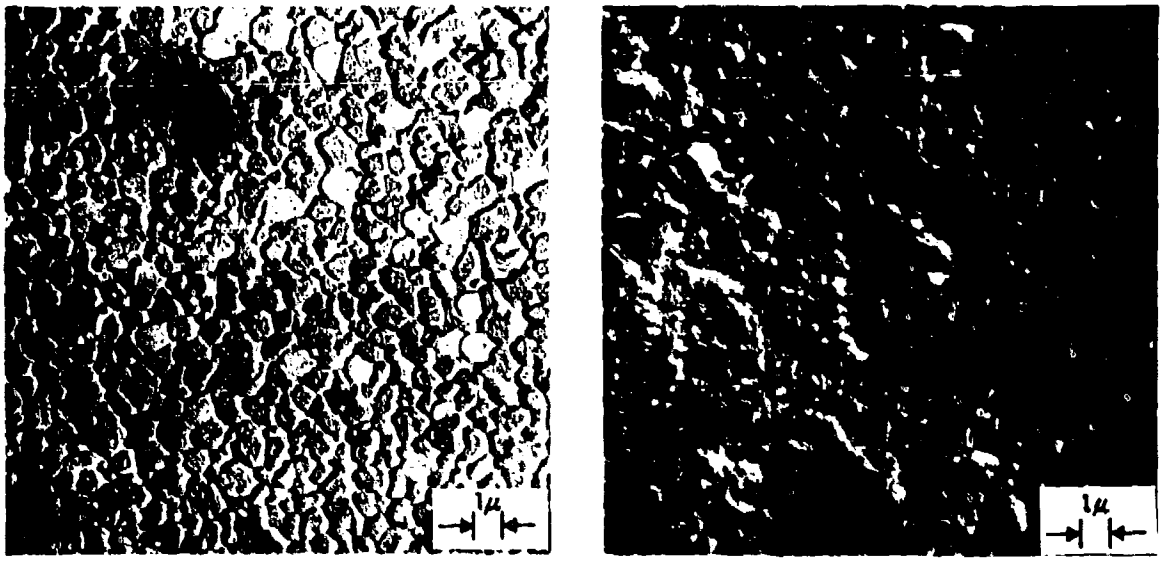

(e). 175°C (f). 200°C

Figure 12 (Continued). Electron Micrographs of AgI Films Deposited at Different Substrate Temperatures

The cell was then charged under 0.5 V. A typical charging current-time curve is shown in Figure 13. The sharp drop-off in charging current is a necessary (but not sufficient) condition for substantial absence of electronic conductivity. A set of discharge curves is shown in Figure 14. The cell exhibits excellent voltage stability when charged to 0.5 V and is currently still in operation. For example after two months of storage one such cell had an open circuit voltage of 0.470 which was identical to the initial OCV value. At that point a check was made of its dc internal resistance by the impedance matching method which revealed an internal resistance of the order of 10^4-10^5 ohm, i.e. same as before. The open circuit voltage after this small drain of charge stabilized at 0.400 to 0.410 V where it has remained since (i.e. approximately 1-1/2 months hence).

We feel, at the moment, that this Ag/evap. AgI, iodized Ag/Pt cell represents the best and most promising approach to our assigned objective: to wit, demonstrates the feasibility of thin-film fabrication of stable, active, rechargeable cells of the type Ag/AgI/Pt.

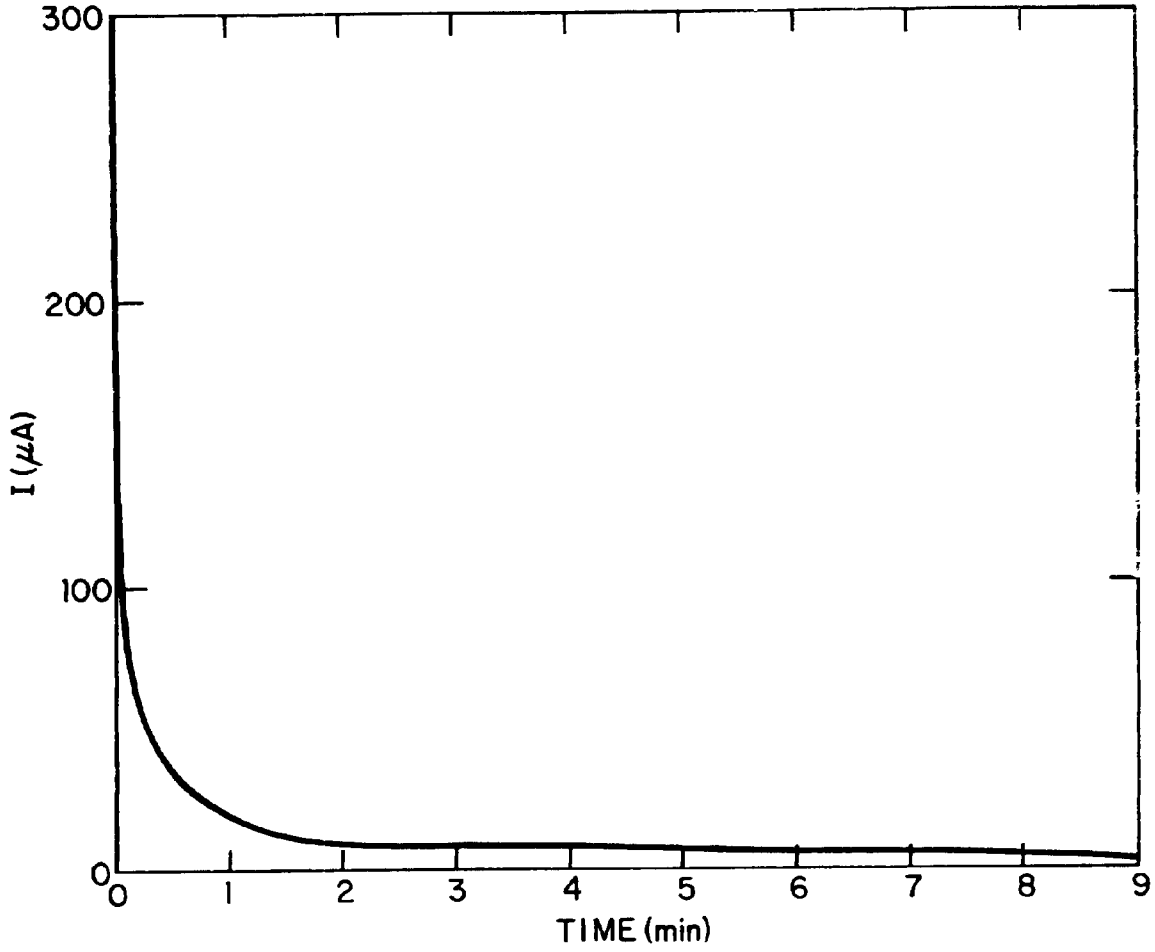

Figure 13. Typical Charging Curve for Overlapping Ag/Evap. AgI, Iodized Ag/Pt Cell

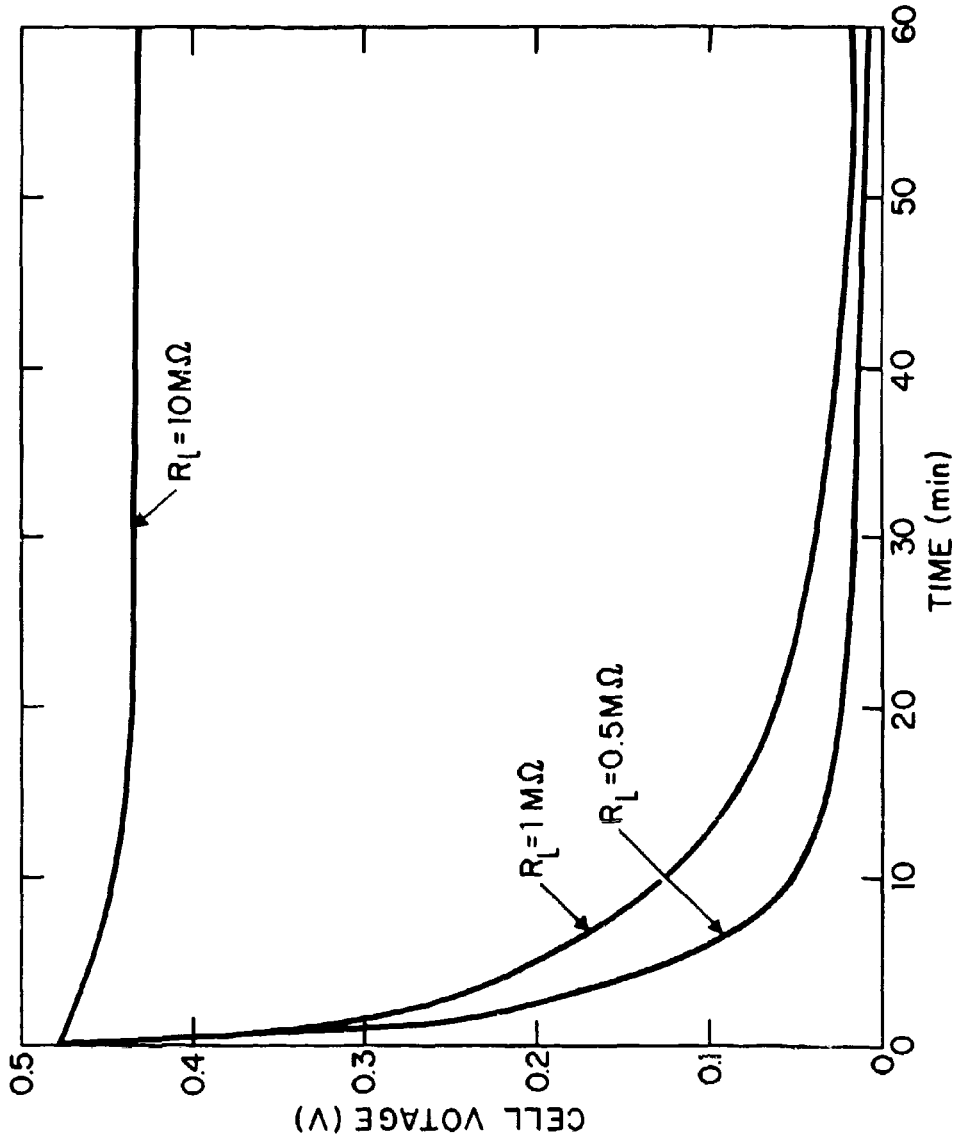

Figure 14. Discharge Curves for Overlapping Ag/Evap. AgI, Iodized Ag/Pt Cell

III. DISCUSSION

A. FUNDAMENTAL NATURE OF THE Ag/AgI/Pt SYSTEM

It has been pointed out (1) that it was found convenient to view the Ag/AgI/Pt system as a solid-electrolyte concentration cell in which the internal driving force is the obviously high concentration of silver in the silver anode working through the ionically conductive AgI against the obviously low concentration of silver in the platinum electrode. If this is so, and if we assume that the fundamental electrochemistry of liquid electrolytes applies to solid electrolytes, the open circuit voltage, E, of the cell should be given by the Nernst equation:

$$E = \frac{RT}{nF} \ln \frac{a_s}{a_p} \ldots , \qquad (1)$$

where R is the gas constant, T is the absolute temperature, n is an integer (in this case unity), F is the Faraday constant, a_s is the (constant) activity of silver in the silver electrode and a_p is the (variable with state of charge) activity of silver in the platinum electrodes. Rearranging, combining terms, and converting to Naparian logarithm, we have that:

$$E = a\left(1 - \log a_p\right) \ldots , \qquad (2)$$

where a is a constant.

As the cell discharges silver is transported to the platinum and the activity, a_p, of silver in the platinum increases. Thus the equilibrium open-circuit voltage, E, of the cell should decrease exponentially with discharge. All of the discharge curves in this report, however, plot the closed-circuit voltage, V, of the cells as a function of time of discharge through a fixed load resistance, R_L. Since V is less than E by an amount corresponding to the total internal IR losses within the discharging cell (and these losses are a function of the amount of charge, q, transported at any time, t, of discharge) our V-T discharge curves cannot be easily interpreted to confirm or disprove the validity of the concentration-cell model.

It is possible that in the charged condition the Ag/AgI/Pt resembles a low-voltage solid-electrolyte capacitor. Or it could be that the charging process, even though it is carried out at voltages (0.5-0.6 V) which are lower than the decomposition voltage of AgI (about 0.68 V), may in fact produce some iodine at the AgI/Pt interface.

Whatever the ultimate model may be, the fact remains that the closed-circuit voltage, unlike that of conventional oxidation-reduction cell systems, does drop exponentially with discharge time.

B. SIGNIFICANCE OF AN EXPONENTIALLY-DROPPING CLOSED-CIRCUIT VOLTAGE

Electronic engineers obviously prefer battery power sources whose closed-circuit voltage is substantially constant. Typical examples are nickel-cadmium and the Ruben-Mallory zinc-mercuric oxide batteries whose discharge curves are practically horizontal and then suddenly drop off. A disadvantage of such a "plateau-discharge" battery system is that a measurement of either the equilibrium or closed-circuit voltage gives no reliable measure of the residual capacity remaining in a partially discharged battery. Measurement of the equilibrium open-circuit voltage of a "concentration-cell" battery or of the closed-circuit voltage across a known load resistance can, on the other hand, be used to estimate residual capacity.

Another possible advantage of a battery system whose closed-circuit voltage is a function of discharge time involves using this OCV as a measure of time — i.e. an electrochemical timer. Reliability could be enhanced by redundancy (e.g., use several cells in parallel). Temperature compensation should present no serious problems. In addition, such batteries with exponential discharge (or charge) curves could, through simple circuitry, be used as current integrators.

C. MINIMIZING THE DROPPING CLOSED CIRCUIT VOLTAGE

These advantages, however, of a "concentration cell" are really not enough to outweigh the advantages of the more constant closed-circuit voltage and increased specific outputs of conventional oxidation-reduction battery systems. One way to minimize the dropping discharge curve of a concentration cell system is to use more anode and, particularly, more cathode material. Thus, in the Ag/AgI/Pt system, a thicker platinum electrode would permit absorption of more silver before the silver activity, a_p (see Eq. (2)),would increase significantly to drop either E, the open-circuit voltage or V, the closed circuit voltage. This improvement was confirmed experimentally in Reference (1).

There are other ways to improve the output capacity of concentration cell systems (more conductive electrolytes like in Section II-D-3 above using a KI/AgI double salt, increased effective anode-electrolyte and cathode-electrolyte contact through dispersion of electrolyte into anode and cathodic materials, etc.).

D. DEVELOPMENT OF THIN-FILM, ALL-SOLID OXIDATION-REDUCTION SYSTEMS

Development of a suitable, vacuum-deposited oxidizing agent to yield stable, rechargeable oxidation-reduction thin-film batteries of the type Ag/AgI/Oxidizing Agent would, in principle, like other oxidation-reduction systems, result in plateau-type discharge curves. This approach would require successful developments of an oxidizing agent which (a) would not react with the AgI (or whatever solid-electrolyte is used), (b) would be capable of absorbing incoming cations (i.e. an ionic conductor), and (c) would be capable of absorbing incoming electrons (i.e. exhibits electronic conductivity). The approach to conditions (b) and (c) would probably involve synthesis of non-stoichiometric evaporable oxidizing agents. This may not be too difficult.

IV. CONCLUSIONS

A. THIN-FILM BATTERIES

The work reported above demonstrates the underlying feasibility of fabrication of stable and rechargeable solid-electrolyte thin-film batteries. Prudence and an awareness of the many unforeseen difficulties which seem inevitable in the development of any new battery system require that this optimistic prognosis be tampered with precaution. It is quite likely that even the best configurations we have assembled to date will prove defective because of any of several reasons (electronic conductivity through non-stoichiometric electrolytes; disappearance of silver films through oxidation, diffusion or electrolyte reaction; loss of recharge capability due to silver tree-formation through thin electrolyte films; a gradually increasing cell resistance with time, etc.). It is felt that these problems are amenable to detection and evaluation and, hence, to solution if and when they come up. As of this moment, it appears that the best approach would be to use the iodized silver system described in Section II-H-3 above.

B. THIN-FILM SENSORS

Symmetrical thin-film arrays of the general type M/MX/M in the nonoverlapping geometry may have numerous civilian and military applications in the area of temperature and deformation sensing. For all practical purposes this field is completely unexplored.

V. RECOMMENDATIONS

The work on thin-film unit cells represents the first step toward the development of thin-film multiple-cell batteries. The next logical step is to select the most promising system, optimize its output characteristics and thoroughly evaluate reproducibility and reliability. The final step would involve design, construction, and run-in of pilot-plant production lines. Adoption of such a long-range, and rather costly, program cannot be recommended until a real need for such batteries can be established. Perhaps the most realistic interim objective would be to concentrate on the development and in-depth evaluation of the best unit cell. This could be done through continuation of a contractual arrangement similar to the one under which this work has been done. Another procedure could be based on a "service" arrangement whereby Technical Operations could supply sample unit cells prepared to USAECOM specifications.

APPENDIX A

ELECTRICAL MEASUREMENTS

INTRODUCTION

We present in this appendix background material to electrical measurements of the evaporated cells described in the preceding text. In this connection, it is useful to consider some simple electrical analogue of a typical Ag/AgX/Pt cell, shown in Figure 15

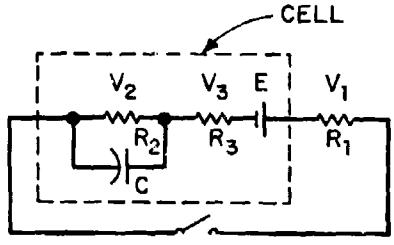

Figure 15. Sample Circuit Analogue of Cell

where R_1 is the load; R_2, the shunted resistance (interfaces); R_3, the unshunted resistance (electrolyte); C, the double layer capacitance; E, the cell's emf (open-circuit voltage); and V_1, the cell voltage. By applying the basic principles stated by Kirchhoff's laws,

$$E = V_1 + V_2 + V_3$$

and

$$V_1\left(\frac{1}{R_1} + \frac{1}{R_2} + \frac{R_3}{R_1R_2}\right) - \frac{E}{R_2} = -C\left(1 + \frac{R_3}{R_1}\right)\frac{dV_1}{dt} \quad ,$$

then

$$V_1 = E\,R_1\left\{\frac{R_1 + R_3 + R_2\, e^{-\left[\left(R_1 + R_2 + R_3\right)/R_2\left(R_1 + R_3\right)C\right]\tau}}{\left(R_1 + R_3\right)\left(R_1 + R_2 + R_3\right)}\right\} \quad . \qquad (3)$$

At $\tau = 0$,

$$V_1 = E R_1/(R_1 + R_3) \quad . \tag{4}$$

At $\tau = \infty$,

$$V_1 = E R_1/(R_1 + R_2 + R_3) \quad . \tag{5}$$

At $\tau = R_2(R_1 + R_3)C/R_1 + R_2 + R_3$, when R_3 is very small, Eq. (3) reduces to

$$V_1 = \frac{E R_1}{R_1 + R_2} \left[1 + \frac{R_2}{R_1} e^{-\left[(R_1 + R_2)/R_1 R_2 C\right]\tau}\right] \quad , \tag{6}$$

and, furthermore, if

$$R_1 >> R_2, \quad \tau \cong R_2 C; \quad R_2 >> R_1, \quad \tau \cong 2R_1 C; \quad \text{and if} \quad R_1 \cong R_2, \quad \tau \cong \frac{RC}{2} \quad .$$

We make no pretense that this circuit exactly simulates a cell. For example, the circuit assumes constant values for C, R_1, R_2, R_3, and E; whereas, in reality, E varies as a function of the concentration of Ag at the Pt electrode, and both R_2 and C undoubtedly depend in a complicated way on E, R_1, and other factors. However, because there are significant similarities in behavior, especially for small time durations during which E may be assumed constant, and for large R_1 which insures a small current drain, the analogue is a useful guide.

Now, an important measurement to make is the origin of cell resistance. The circuit analogue suggests that the cell's dc resistance can be quickly checked by first charging the cell, then measuring V_1 with a high impedance voltmeter (equivalent to an open circuit voltage measurement for which $R_1 \rightarrow \infty$ and $V_1 = E$), and finally repeating the measurement with a finite load R_1 chosen such that $V_1 = E/2$. The dc cell resistance $R_2 + R_3$, in accordance with Eq. (5), is then equal to the load R_1. Although the cell inadvertently runs down during this type of measurement, R_1 is large enough so that the current drain is modest and a good estimate can be made. The circuit analogue also suggests that, if the resistance R_2 presumably associated with the electrodes is mostly shunted by a double layer capacitance C, then the unshunted resistance R_3, primarily the electrolyte resistance, can be measured or at least bounded with an ac bridge in which the cell's emf = E is biased out, the load R_1 is removed, and the ac frequency f is high enough to make the capacitive impedance $1/2\,\pi fc$ much smaller than R_3.

We have reported both types of measurements on our AgX cells which show that the audiofrequency ac cell resistance is typically at least 2 orders of magnitude smaller than the dc cell resistance. This large ratio is a significant finding, indicating that a large part of the internal resistance is indeed effectively shunted by a very large double layer capacitance ($10^2 - 10^3 \mu F$). Since the interelectrode capacitance ($\sim 10^{-3} \mu F$) is negligible, we learn from our ac and dc measurements that the observed capacitance and, hence, the shunted internal resistance must be associated with the electrode-electrolyte interfaces. It follows that the unshunted resistance of the ac measurement must consist of the electrolyte resistance plus any contribution from the interface resistance that is ineffectively shunted. Thus the ac resistance can be considered as an upper bound on the electrolyte resistance. As such, it is unwise to denote the ac values as a basic measurement of specific electrolyte conductivity. Yet these values are small enough to show that an evaporated layer of a very high resistivity ionic conducting material can, per se, be a relatively low resistance element in a cell, i.e., we can assume that $R_3 << R_2$ in our circuit analogue applied. Because of structural factors which might yield an undesirably large resistance in an evaporated film, this was not taken for granted simply because the layer is thin.

Curves of cell voltage V_1 vs time (describing the discharge of charged AgBr and AgI cells into various loads) show that, for concentration cells of large capacity, such as the pellets reported by Mrgudich,* where a large enough load resistor was used to prevent severe current drain, the discharge curves for various loads fall as a transient from the voltage $V_1 = E$ as predicted by Eq. (4) in which $R_3 << R_1$. This transient is due to polarization effects or double layer charging as suggested by Eq. (6). After this initial transient, the curves tend to level off similar to the Eq. (7) curves. For concentration cells of lower capacity, such as evaporated cells, the initial voltage drop is also a transient starting from $V_1 = E$ since $R_3 << R_1$. However, for the smaller values of R_1, such as 0.5 MΩ in Figure 6, of the main report, the current drain causes a continuous voltage drop and the curves do not level off. Because of the choice of such high load resistances for the evaporated cells, the electrolyte is too small a resistance to have any voltage effect on the discharge curves, and no measurement of R_3 can be made from these curves.

For the discharge curves of the pellet batteries, $R_1 \geq 0.1$ MΩ. Thus, from Eq. (6) the initial voltage drop from $V_1 = E$ is characterized by a slope E/τ or a time constant in the range $\tau = R_2C \rightarrow R_1 C/2$, which may be on the order of a second. Since the traces are recorded on a horizontal time scale of 10 min/div, the initial voltage drop is not well resolved, i.e., although the curves for various loads ($R_1 >> R_3$) all start from the same $V_1 = E$ intercept in accordance with Eq. (4), the initial polarization voltage drop in the case of the smaller load resistance (for which the time constant of the initial drop is smaller) appears to be instantaneous rather than of finite slope. For the evaporated batteries, this effect is somewhat less pronounced because of what appears to be a greater time constant in the polarization of the double layer. This is undoubtedly a result of the larger electrode interface resistance and capacitance associated with the evaporated cell. As reported by Raleigh, the time constant associated with the polarization transient is not single valued, but may have 2 or 3 different values during the transient due to various electrode processes.

*J. N. Mrgudich et al. Trans. IEEE AES-1, 295 (1965).

With these facts in mind, let us now proceed to discuss the performance characteristics of the thin-film cells prepared under this program.

AC AND DC CHARACTERISTICS OF THIN-FILM CELLS

It is clear from the foregoing discussion that the relatively high dc internal resistance of the thin-film cells is almost in its entirety due to boundary factors.

Two methods of boundary analysis have recently been employed with thick, pellet-type systems. In the first, both electrodes were made of the same metal[14] and ac bridge measurements were performed. In the second, a small probe, or third electrode wire, was introduced into the electrolyte.[15,16] The probe electrode drew negligible current, but was used to study the response of each electrode interface to a small dc voltage step impulse applied across the cell. Although the methods should yield equivalent results, a comparison of the two investigations shows considerable disagreement in the measured values of interface capacitance. The need for further research is indicated; nevertheless, similar boundary analysis studies carried out with evaporated systems provide an important contribution.

Since little information is currently available about the conductivity of evaporated silver halide films, it was necessary to develop techniques to measure the resistance of the thin-film electrolytes and the electrical properties of the electrode-electrolyte boundaries. The first step was the extension of methods that are well known in solid-state electrochemistry to thin films. These methods include the application of the dc voltage steps and ac resistance and capacitive bridge measurements. A dc measurement of Ag/AgBr/Pt or Au cells shows that the internal resistance is on the order of $10^5\,\Omega$. If an ac resistance bridge (Figure 16) measurement is made with a small ac signal voltage (1 to 100 kcps) impressed across the cell, measured values are less than 100 Ω. The ac resistance values drop slightly with frequency, and they are found to be independent of frequency above 20 kcps (see Table 1).

The phenomenon of a buildup of a capacitive double layer, C, when step voltages are applied to a cell is illustrated in Figure 17. Here, for convenience, we employ an Ag/AgBr/Ag overlapping configuration with symmetric reversible electrodes. A 10 mV step is applied to this cell through load resistors, $R = 10^3$, 10^4, 10^5, and $10^6\,\Omega$, and the circuit current is recorded. Both the initial or "flash current" values, i_o, and the asymptotic current values, i_s, of Figure 17 are found to fit a simple circuit analogue and its equation within 10% (see Figure 15) where the dc resistance of the cell is evaluated at $r = 1.1 \times 10^4\,\Omega$ plus a small contribution from the electrolyte, r_e. Raleigh,[16] in a high temperature study of pellet systems, has shown that the capacitive double-layer value is not single valued but depends somewhat on cell voltage. This is suggested here (Figure 17) by the fact that the curves do not appear to be purely exponential; also, the curves indicate that C is on the order of $10^3\,\mu F$, roughly in agreement with Raleigh's results. (These results do not agree with those of Friauf,[14] however. By using the same symmetric Ag/AgBr/Ag combination in pellet form, Friauf obtains double-layer capacitive values orders of magnitude lower. In addition, he gives nearly equal ac and dc resistance values, which are in disagreement with our measurements.*)

*These discrepancies may be due to sample impurities in which charge carriers other than Ag^+ are involved

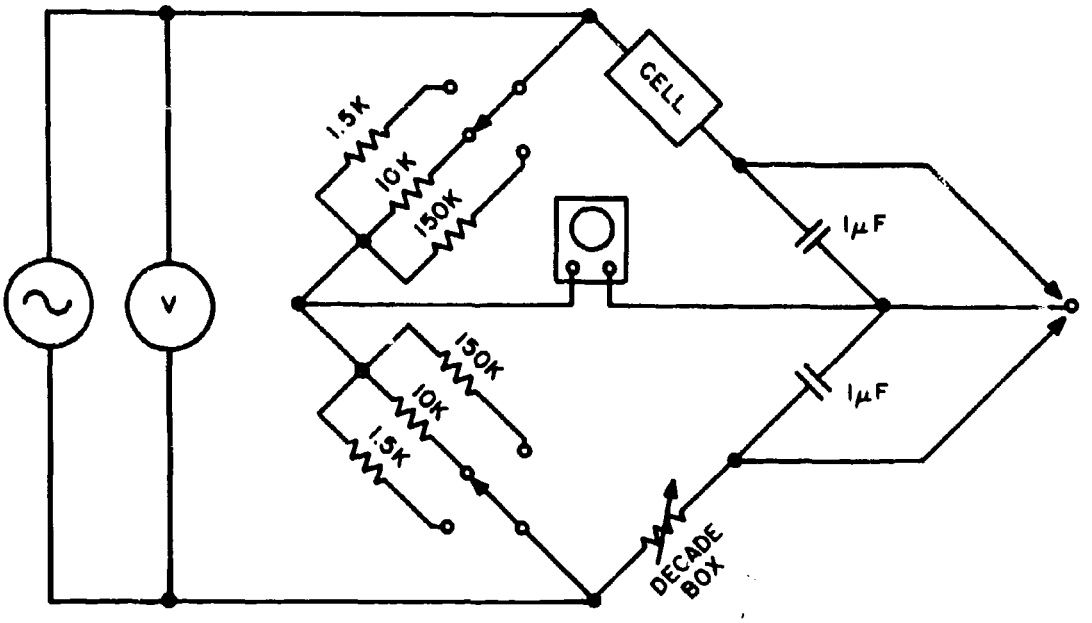

Figure 16. AC Bridge for Conductivity Measurements

TABLE 1

AC RESISTANCE VALUES OF AN Ag/AgBr/Au CELL AS A FUNCTION OF FREQUENCY*

Frequency (kcps)	Resistance (Ω)	
	25 Ω Resistor	AgBr Film†
0.01	–	60-70
0.10	26	30
1.0	26	20
10	26	20
100	26	18
200	26	18
500	–	17
600	22	–

*If cell is charged, it must be prevented from discharging with a suitable dc bias voltage. In order to av[illegible] the use of a dc bias voltage, the measurements given in Table 1 were made on a symmetrical Ag/AgBr/Ag system.

†The values given in this column have not been corrected for any residual unshunted boundary effects. Electrolyte thickness is 10 μ.

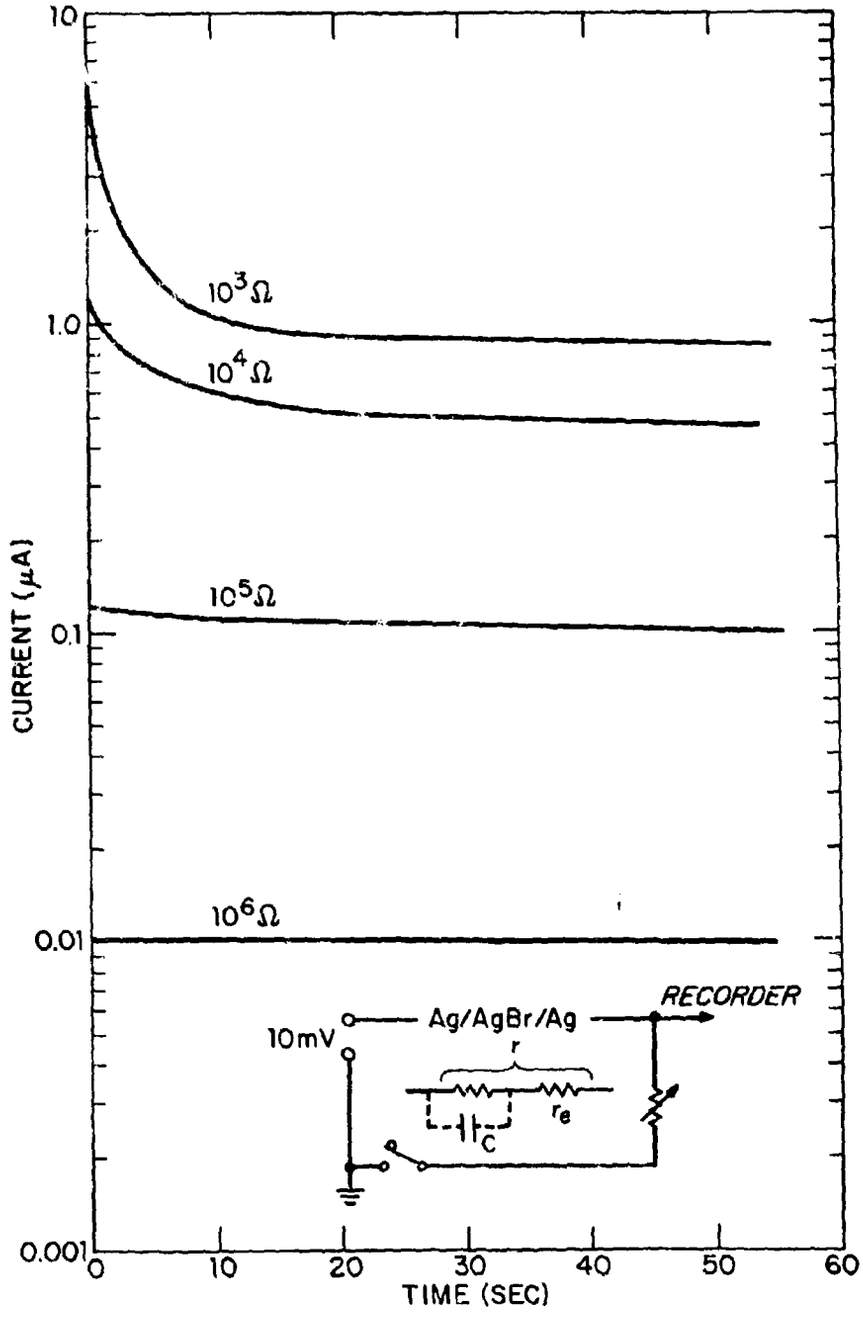

Figure 17. Transient Response of an Ag/AgBr/Ag Thin-Film System to a 10 mV Step Using Various Loads Large Compared with Electrolyte Resistance

The sample's interface capacitance should appear as a significant reactance ($R_c = 1/2\,\pi fC$) in an ac measurement of the sample at frequencies below 100 kcps. Because a purely resistive bridge cannot be properly balanced in the presence of an appreciable capacitive reactance in the sample, Table 1 shows an increase in the effective ac resistance due to R_c as the frequency decreases below 100 kcps. The higher frequency value of resistance (18 and 17 Ω) should be considered, therefore, as representative of the electrolyte resistance plus any unshunted interface resistance. From this we can place an upper bound on a specific ionic conductance of $1.4 \times 10^{-4}\ \Omega^{-1}\ cm^{-1}$ for the evaporated AgBr film based on a film thickness of 10 μ and an electrode overlap area of 0.4 cm^2. Other bulk conductivity measurements[17] have demonstrated that the σ values vary from $\sim 2 \times 10^{-7}$ to $\sim 2 \times 10^{-5}\ \Omega^{-1}\ cm^{-1}$, which at its highest is 10 times lower than our upper bound on evaporated AgBr films. A comparison of bulk and thin-film conductivity values, however, may be unrealistic since the bulk AgBr measurements were made at room temperature where the distribution of Frenkel defects are to a large degree a function of sample preparation techniques. A more reasonable comparison would be made at elevated temperatures where the Frenkel defects in the electrolyte are more randomly distributed and are independent of sample preparation.

The specific conductance of the evaporated AgI films was also estimated as an upper bound by the ac method. The resistance variation of the film with the applied voltage frequency is shown in Table 2 for a film of thickness of 44 μ and an electrode overlap area of 0.4 cm^2. We can calculate the specific conductance of evaporated AgI films using the resistance reading at the highest frequency. The calculated value of σ_{AgI} is $1.1 \times 10^{-3}\ \Omega^{-1}\ cm^{-1}$, which is roughly 10 times higher than that of evaporated AgBr films.

TABLE 2

RESISTANCE VALUES OF EVAPORATED AgI FILM

Frequency (kcps)	Electrolyte Resistance* (Ω)
600	10
300	30
100	120
10	200
1	220
0.1	280

*All values corrected for the resistance of the Pt films. Electrolyte thickness is 44 μ.

CONCLUDING REMARKS

We have shown that the internal resistance of a cell can influence its ultimate performance, and it is therefore of major importance to examine the sources and causes of the high internal resistance of thin-film batteries. Basically, the conditions that contribute to these high resistance values have been found to be due almost entirely to boundary conditions at either one or both of the electrode-electrolyte interfaces.

The results presented and discussed in the preceding sections lead us to recommend that more definitive experiments* be conducted in the future in which a variation of double layer capacitance (with frequency) is studied. For example, the observed decrease of ac resistance values with frequency differed for AgI and AgBr data. The AgBr data showed little drop with frequency above 1 kcps. The AgI data showed a much greater reduction. This type of dispersion data could give some indication as to the kinetics at the electrode interface.

It would also be valid to consider pulse measurements to substitute for ac measurements since in principle they are, of course, equivalent. In the pulse method a small charging voltage pulse is applied to the cell and the current response is measured, or the cell in some state of charge is rapidly switched into an external circuit (flash current method) and the initial current is measured. In either case, the impedance of the external circuit including pulse voltage source must clearly not be much larger than the unshunted cell resistance. The switching speed determines the equivalent bandwidth of the excitation, and the recording equipment must be fast enough to respond to the leading edge of the current pulse. The ac method appears to have the advantage of simple equipment requirements, but the pulse method has the advantage of minimal perturbation of the physical state of the cell.

Finally, in retrospect it would have been proper to consider taking discharge curves with much smaller load resistances of the order of the electrolyte resistance. This amounts to a pulse discharge method or flash current method equivalent to an ac resistance measurement as mentioned above. (Our ac measurements using the ac bridge in Figure 16 indicate that a load resistance in the 10-100 Ω range or less would be needed.) In this case the discharge curves would not all start at the same $V_1 = E$ intercept, but from a point V_1 on the voltage scale depending on R_3, as given by Eq. (4). The resistance R_3 could then be calculated from this simple equation. The accuracy in the determination of V_1 at time zero, however, depends on the switching speed of the discharge circuit, the response speed of the recorder or scope, and on the accuracy of extrapolation of the discharge curve to establish the actual time zero voltage intercept. These factors make up the equivalent bandwidth of the pulse method. In a cell with an unshunted resistance R_3 and a load R_1, both equal to about 10 Ω, and a double layer capacitance C estimated as 100 μF, Eq. (3) gives approximately 10^{-4} sec as the time for the voltage to drop by about 10% from its t = 0 value as given in Eq. (4). It would,

*See, for example, D.O. Raleigh, J. Phys. Chem. 70 (1966).

then, seem that the switching time and recorder response time should each be less than 10^{-4} sec. The value R_3 obtained from Eq. (4) by the discharge pulse or flash current method is subject to the same interpretation as the ac cell resistance measurement, i.e. R_3 would appear to consist of the electrolyte resistance plus a contribution from electrode interface resistance that is unshunted during the initial current in the circuit. Therefore, at best it would be an upper bound on the resistance of the electrolyte.

REFERENCES

1. J.N. Mrgudich, P.J. Bramhall, and C.M. Schwartz, "Army Science Conference Proceedings" (Available through Clearinghouse of Federal Scientific and Technical Information, Dept. of Commerce, Springfield, Virginia 22151, 1966), Vol. 2, p. 127.

2. J.N. Mrgudich, "Army Science Conference Proceedings" (To be available through Clearinghouse of Federal Scientific and Technical Information, Dept. of Commerce, Springfield, Virginia 22151, 1968. A preliminary report on ionic sensors was presented at the 21st Power Sources Conference, p. 117, 1967).

3. Radio Corporation of America, Scientific American 218 (3), 17 (March 1968).

4. D.O. Raleigh, "Solid State Electrochemistry," in Progress in Solid State Chemistry (New York, N.Y.: Pergamon Press, 1966), Vol. 3.

5. J.N. Mrgudich, "Solid Electrolyte Batteries," in Encyclopedia of Electrochemistry, edited by C.A. Hampel (New York, N.Y.: Reinhold, 1964), p. 84.

6. D.V. Louzos, U.S. Pat. 2,894,053, July 7, 1959; G.F. Evans, U.S. Pat. 2,894,052, July 7, 1959; J.J. Buchinski, et al., U.S. Pat. 2,932,569, April 10, 1960; D.V. Louzos, Battery Division Extended Abstracts, Boston Meeting, Electrochemical Society, 1962, p. 88.

7. A. Shepp, G. Goldberg, J. Masters, and R. Lindstrom, Phot. Sci. Eng. 11, 316 (1967).

8. J.N. Bradley and P.D. Greene, Trans. Faraday Soc. 62, 2069 (1966); 63, 2516 (1967).

9. B.B. Owens and G.R. Argue, Science 157, 308 (1967).

10. S. Geller, Science 157, 310 (1967).

11. G.R Argue, B.B. Owens, and I.J Grace, "Solid-Electrolyte Batteries," presented at Power Sources Conference, Atlantic City, 16 May 1968.

12. R.N. Schock and S. Katz, J. Chem. Phys. 48, 2094 (1968).

13. C.M. Perrott and N.H. Fletcher, J. Chem. Phys. 48, 2143 (1968).

14. R.J. Friauf, J. Chem. Phys. 22, 1329 (1954).

15. D.O. Raleigh, J. Phys. Chem. 70, 689 (1966).

16. D.O. Raleigh, J. Phys. Chem. 71, 1785 (1967).

17. I. Shapiro and I.M. Kolthoff, J. Chem. Phys. 15, 41 (1947).

Unclassified

Security Classification

DOCUMENT CONTROL DATA - R&D

(Security classification of title, body of abstract and indexing annotation must be entered when the overall report is classified)

1. ORIGINATING ACTIVITY *(Corporate author)*
Technical Operations, Incorporated
Burlington, Massachusetts

2a. REPORT SECURITY CLASSIFICATION
Unclassified

2b. GROUP
--

3. REPORT TITLE

Fabrication of Ultrathin Solid Electrolyte Batteries

4. DESCRIPTIVE NOTES *(Type of report and inclusive dates)*
Final report April 1967 to March 1968

5. AUTHOR(S) *(Last name, first name, initial)*

Vouros, P., Clune, J., and Masters, J.I.

6. REPORT DATE	7a. TOTAL NO. OF PAGES	7b. NO. OF REFS
August 1968	36	17

8a. CONTRACT OR GRANT NO.	9a. ORIGINATOR'S REPORT NUMBER(S)
DAAB 07-67-C-0339	TO-B 68-31
b. PROJECT AND TASK NO.	
c. DOD ELEMENT	9b. OTHER REPORT NO(S) *(Any other numbers that may be assigned this report)*
d. DOD SUBELEMENT	ECOM-0339-F

10. AVAILABILITY/LIMITATION NOTICES This document is subject to special export controls and each transmittal to foreign governments or foreign nationals may be made only with prior approval of CG, U.S. Army Electronics Command, Fort Monmouth, N.J. Attn: AMSEL-XL-E

11. SUPPLEMENTARY NOTES	12. SPONSORING MILITARY ACTIVITY
	U.S. Army Electronics Command Fort Monmouth, New Jersey

13. ABSTRACT

The objective of this study was to determine the feasibility of preparing solid-electrolyte batteries using only vacuum-deposited thin films. This feasibility has been demonstrated. Batteries were made in two configurations (nonoverlapping and overlapping electrodes). In all cases the anode material was an evaporated Ag film; a variety of electrolytes were studied (evaporated AgI, co-evaporated AgI and KI, evaporated AgBr, a double electrolyte of AgI evaporated onto a film of evaporated AgCl, a double electrolyte of AgI evaporated onto a film of AgI prepared by iodizing a thin film of Ag previously evaporated onto a film of sputtered Pt); cathode materials were sputtered Pt films (usually) or evaporated Au. Overall cell thicknesses were in the range of 6-12 microns. Preliminary tests indicate that such thin cells are rechargeable and some are apparently of long shelf-life.

DD FORM 1 JAN 64 1473

Unclassified

Security Classification

Security Classification

14. KEY WORDS	LINK A		LINK B		LINK C	
	ROLE	WT	ROLE	WT	ROLE	WT

INSTRUCTIONS

1. ORIGINATING ACTIVITY: Enter the name and address of the contractor, subcontractor, grantee, Department of Defense activity or other organization *(corporate author)* issuing the report.

2a. REPORT SECURITY CLASSIFICATION: Enter the overall security classification of the report. Indicate whether "Restricted Data" is included. Marking is to be in accordance with appropriate security regulations.

2b. GROUP: Automatic downgrading is specified in DoD Directive 5200.10 and Armed Forces Industrial Manual. Enter the group number. Also, when applicable, show that optional markings have been used for Group 3 and Group 4 as authorized.

3. REPORT TITLE: Enter the complete report title in all capital letters. Titles in all cases should be unclassified. If a meaningful title cannot be selected without classification, show title classification in all capitals in parenthesis immediately following the title.

4. DESCRIPTIVE NOTES: If appropriate, enter the type of report, e.g., interim, progress, summary, annual, or final. Give the inclusive dates when a specific reporting period is covered.

5. AUTHOR(S): Enter the name(s) of author(s) as shown on or in the report. Enter last name, first name, middle initial. If military, show rank and branch of service. The name of the principal author is an absolute minimum requirement.

6. REPORT DATE: Enter the date of the report as day, month, year, or month, year. If more than one date appears on the report, use date of publication.

7a. TOTAL NUMBER OF PAGES: The total page count should follow normal pagination procedures, i.e., enter the number of pages containing information.

7b. NUMBER OF REFERENCES: Enter the total number of references cited in the report.

8a. CONTRACT OR GRANT NUMBER: If appropriate, enter the applicable number of the contract or grant under which the report was written.

8b, 8c, & 8d. PROJECT NUMBER: Enter the appropriate military department identification, such as project number, subproject number, system numbers, task number, etc.

9a. ORIGINATOR'S REPORT NUMBER(S): Enter the official report number by which the document will be identified and controlled by the originating activity. This number must be unique to this report.

9b. OTHER REPORT NUMBER(S): If the report has been assigned any other report numbers *(either by the originator or by the sponsor)*, also enter this number(s).

10. AVAILABILITY/LIMITATION NOTICES: Enter any limitations on further dissemination of the report, other than those imposed by security classification, using standard statements such as:

(1) "Qualified requesters may obtain copies of this report from DDC."

(2) "Foreign announcement and dissemination of this report by DDC is not authorized."

(3) "U. S. Government agencies may obtain copies of this report directly from DDC. Other qualified DDC users shall request through _____."

(4) "U. S. military agencies may obtain copies of this report directly from DDC. Other qualified users shall request through _____."

(5) "All distribution of this report is controlled. Qualified DDC users shall request through _____."

If the report has been furnished to the Office of Technical Services, Department of Commerce, for sale to the public, indicate this fact and enter the price, if known.

11. SUPPLEMENTARY NOTES: Use for additional explanatory notes.

12. SPONSORING MILITARY ACTIVITY: Enter the name of the departmental project office or laboratory sponsoring *(paying for)* the research and development. Include address.

13. ABSTRACT: Enter an abstract giving a brief and factual summary of the document indicative of the report, even though it may also appear elsewhere in the body of the technical report. If additional space is required, a continuation sheet shall be attached.

It is highly desirable that the abstract of classified reports be unclassified. Each paragraph of the abstract shall end with an indication of the military security classification of the information in the paragraph, represented as *(TS), (S), (C), or (U).*

There is no limitation on the length of the abstract. However, the suggested length is from 150 to 225 words.

14. KEY WORDS: Key words are technically meaningful terms or short phrases that characterize a report and may be used as index entries for cataloging the report. Key words must be selected so that no security classification is required. Identifiers, such as equipment model designation, trade name, military project code name, geographic location, may be used as key words but will be followed by an indication of technical context. The assignment of links, rules, and weights is optional.

Security Classification